

Self-Assembly of Left- and Right-Handed Molecular Screws

Fei Xu,[†] I. John Khan,[†] Kenneth McGuinness,[†] Avanish S. Parmar,[†] Teresita Silva,[†] N. Sanjeeva Murthy,[‡] and Vikas Nanda^{*,†}

[†]Center for Advanced Biotechnology and Medicine, Department of Biochemistry and Molecular Biology, Robert Wood Johnson Medical School, Rutgers University, Piscataway, New Jersey 08854, United States

[‡]New Jersey Center for Biomaterials, Piscataway, New Jersey 08854, United States

S Supporting Information

ABSTRACT: Stereoselectivity is a hallmark of biomolecular processes from catalysis to self-assembly, which predominantly occur between homochiral species. However, both homochiral and heterochiral complexes of synthetic polypeptides have been observed where stereoselectivity hinges on details of intermolecular interactions. This raises the question whether general rules governing stereoselectivity exist. A geometric ridges-in-grooves model of interacting helices indicates that heterochiral associations should generally be favored in this class of structures. We tested this principle using a simplified molecular screw, a collagen peptide triple-helix composed of either L- or D-proline with a cyclic aliphatic side chain. Calculated stabilities of like- and opposite-handed triple-helical pairings indicated a preference for heterospecific associations. Mixing left- and right-handed helices drastically lowered solubility, resulting in micrometer-scale sheet-like assemblies that were one peptide-length thick as characterized with atomic force microscopy. X-ray scattering measurements of interhelical spacing in these sheets support a tight ridges-in-grooves packing of left- and right-handed triple helices.

In *Through the Looking Glass*, a fictional account of a mirror-image world, Lewis Carroll presaged our current understanding of biomolecular stereoselectivity suggesting, “Perhaps looking glass milk isn’t good to drink ...”. Mirror-image stereoisomers of proteins, sugars, and other chiral biomolecules would be useless and possibly poisonous to us, due to the inability of our stereoselective enzymes to metabolize these compounds. The inability of endogenous proteases to degrade non-natural stereoisomers can also be used to our advantage, such as increasing the *in vivo* half-life of therapeutic peptides by judicious incorporation of D-amino acids.

Although natural proteins tend to prefer self or homochiral molecular recognition, this is not an absolute rule. Synthetic polypeptides exhibit no consistency in stereoselectivity (Table 1). This lack of consensus suggests that in many cases, detailed aspects of interactions govern recognition.

Despite this, general rules that relate shape complementarity to association would be useful in guiding molecular design. One such rule describes interactions between like- vs opposite-handed helical objects. A geometric analysis of the packing of coiled coils predicted that columnar associations between opposite-handed

Table 1. Preferred Homo- And Heterochiral Associations in Mixtures of Protein Sequence Enantiomers

system	structure	preference
poly L + D-lysine	α -helix	opposite ⁶
self-replicating peptides	α -helix	like ⁷
membrane peptides	α -helix	both ⁸
hydrophobic dipeptides	β -sheet	like ⁹
ambidextrous peptides	α -helix	opposite ¹⁰
enzyme + substrate	α/β -fold	like ¹¹
racemic crystals	various	both ¹²

supercoils would allow for an overall tighter packing density and a greater number of intermolecular contacts than like-handed associations.¹ Optimal packing of like-handed threaded rods requires rotation of principle axes of adjacent rods, preventing tight columnar packing;² this same phenomenon determines helix packing in proteins.³ Molecular simulations of opposite- and like-handed poly alanine α -helices demonstrate a preference for left-right helical dimers.⁴ All of these studies support a general rule that supramolecular interactions of opposite-handed helices will be favored over like-handed assemblies. However, it is challenging to develop an appropriate experimental system that evaluates shape complementarity without being strongly influenced by the details of intermolecular interactions. Ridges-in-grooves interactions have been demonstrated on a macroscopic scale between left- and right-handed bolts.⁵ At the molecular scale, a ‘chemically nude’ system is needed where the shape is a primary factor promoting close packing.

The collagen mimetic peptide (PPG)₁₀ (P = proline, G = glycine) is a promising minimal system for evaluating the role of helix handedness on intermolecular association. Collagen is composed of three chains that are supercoiled to form a triple helix. Except for glycine, all naturally occurring amino acids are levorotatory (L) stereoisomers. Using dextrorotatory (D) stereoisomers results in a mirror-image, opposite-handed triple-helix (Figure 1a). In the collagen mimetic peptide, (PPG)₁₀, proline side chains form the ridges and grooves of the triple-helix. Due to the cyclic aliphatic side chain, one might expect reduced contributions from side chain flexibility, charge-pair interactions, or hydrogen bonding that could influence molecular packing specificity. This leaves the complementary shape of the binding interface as the primary determinant for effective packing.

Received: October 17, 2013

Published: November 27, 2013

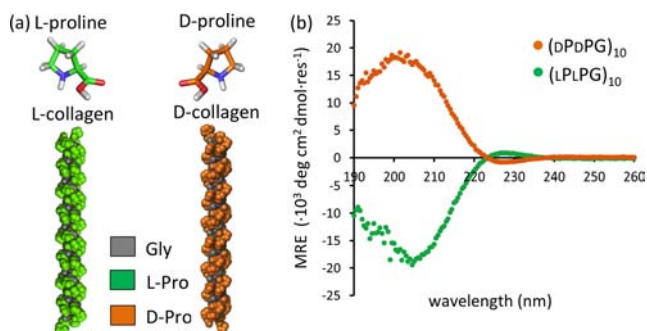


Figure 1. Mirror-image triple helices. (a) Structural models of $[(LPLPG)_{10}]_3$ and $[(DPPD)_{10}]_3$ triple helices. The $[(LPLPG)_{10}]_3$ model was obtained from a high-resolution (1.30 Å) X-ray crystal structure (PDB: 1K6F) 19. (b) CD spectra at 4 °C. $[(LPLPG)_{10}]_3$ and $[(DPPD)_{10}]_3$ refer to triple helices comprised of 3 chains with 10 repeating units of PPG.

Supramolecular assembly of collagen is also of interest due to its favorable properties as a biomaterial. Due to pathological and immunological issues with natural collagen,¹³ bottom-up design of synthetic collagen biomaterials has drawn much attention. Current design strategies utilize noncovalent driving forces such as electrostatics,^{14,15} hydrophobic interactions,^{16,17} and metal-chelating interactions¹⁸ to induce supramolecular assembly of short synthetic collagen mimetic peptides. In this work, the additional contributions of stereochemistry and shape complementarity are explored.

Computational models. $(LPLPG)_{10}$ and its sequence stereoisomer, $(DPPD)_{10}$, both form triple helices with the identical solubility and thermal stability but opposite helical handedness as detected with circular dichroism (Figures 1, S2). The $(LPLPG)_{10}$ peptide forms a right-handed supercoil as shown by its X-ray crystal structure.¹⁹ However, when three chains associate, proline side chains form a continuous, left-handed ridge. We therefore use the convention in this study where $[(LPLPG)_{10}]_3$ forms a left-handed helix and $[(DPPD)_{10}]_3$ forms a right-handed one. Mixed heterotrimers of $(LPLPG)_{10}$ and $(DPPD)_{10}$ could not readily form as this would require proline residues to adopt highly hindered backbone conformations.

Short-range van der Waals interactions between two like- or opposite-handed triple helices were calculated for a series of structures specified by sampling rigid-body translational and rotational degrees of freedom²⁰ (for details of the calculations see Supporting Information and Figure S1). Parallel ($\Omega = 0^\circ$) or antiparallel ($\Omega = 180^\circ$) orientations of the molecular principle axes had optimal contact interfaces as manifested by the lowest interaction scores (Figure 2a). In parallel and antiparallel states, left/right packing was more favorable than left/left packing. Thus, the model predicts that triple helical grooves of opposite-handed molecules interdigitate and interact more tightly and have a shorter optimal interhelical distance than like-handed ones (Figure 2b,c and Table S1). Ridges of two left-handed triple helices were predicted to align by forming edge-to-edge packing, consistent with the lattice packing in X-ray crystal structures of related collagen peptides.²¹

Association stoichiometry. Previous studies of collagen peptide aggregation¹⁶ showed that $(LPLPG)_{10}$ was soluble at very high concentrations (14 mg/mL or 5.5 mM). We observed the same behavior, with similar concentrations of both $(LPLPG)_{10}$ and $(DPPD)_{10}$ remaining in solution for several weeks. Mixing the two sequence stereoisomers induced rapid

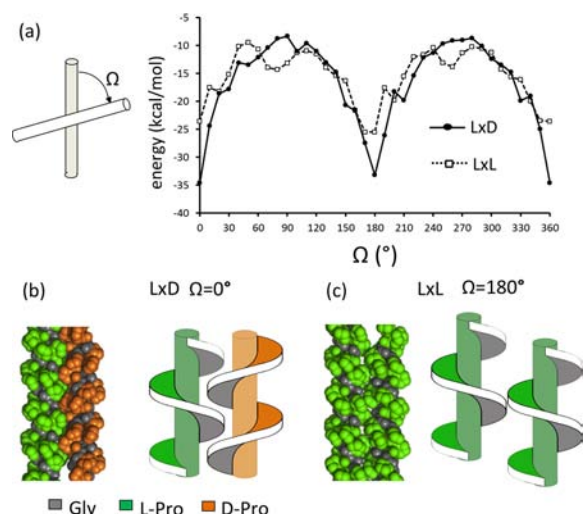


Figure 2. Computational models of opposite ($L \times D$) and like ($L \times L$) packing of collagen triple helices. (a) For each crossing angle, Ω , the packing conformation was optimized and the lowest interaction energy was plotted against Ω . (b,c) Optimal packing conformations of the $L \times D$ and $L \times L$.

aggregation over the course of a few hours (Figure 3). This indicates that supramolecular assembly was facilitated by the presence of opposite-handed species.

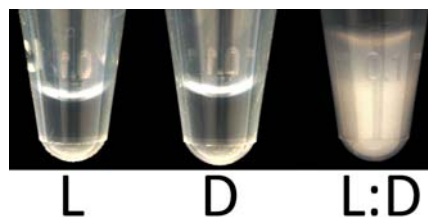


Figure 3. Solubilities of like- and opposite-handed collagen mixtures. L = 5.5 mM $(LPLPG)_{10}$, D = 5.5 mM $(DPPD)_{10}$, L:D = 2.75 mM $(LPLPG)_{10}$ + 2.75 mM $(DPPD)_{10}$. Samples prepared in 10 mM phosphate buffer at pH 7.

To establish whether aggregates were composed of both enantiomers or whether one catalyzed condensation of the other, rates and extents of assembly were measured at a series of concentrations of the D-enantiomer, while keeping the L-enantiomer concentration fixed. A 1:1 mixture rapidly assembled with significant precipitation exceeding the detection limit of static/dynamic light scattering (SLS/DLS) after ~ 8 h (Figure 4). Reduction of the relative concentration of the $(DPPD)_{10}$ species prolonged nucleation times and decreased total scattering intensity indicating less aggregate was made, consistent with a precipitate phase that incorporates both enantiomers.

Morphology of the supramolecular assemblies was observed by transmission electron microscopy (TEM) for various mixing ratios of $(LPLPG)_{10}:(DPPD)_{10}$. The equimolar mixture formed well-ordered micrometer-scale sheets (Figures 5a, S3). Atomic force microscopy (AFM) measurements of these sheets had an average single layer thickness of ~ 10 nm (Figure 5b), which is consistent with the length of a 30-residue triple helix.¹⁹ These heterochiral triple helices may align to form the sheet-like structure (Figure 5c), although higher-resolution data would be needed to confirm this model. This is similar to macroscale assemblies observed in mixtures of millimeter-sized bolts with

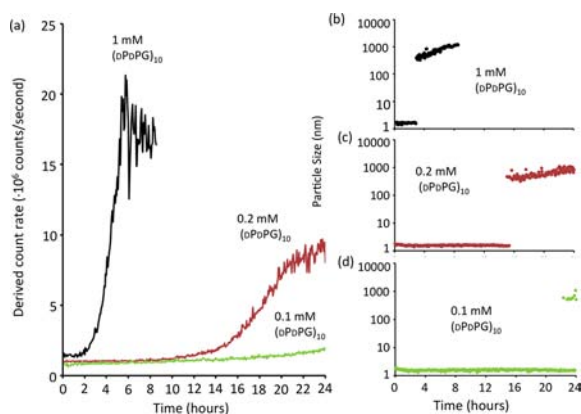


Figure 4. Depleting the D-enantiomer slows aggregation and reduces the total amount formed. (a) Total scattering intensity of a fixed concentration, 1 mM $(L)P(L)PG)_{10}$, combined with 1, 0.2, and 0.1 mM $(D)P(D)PG)_{10}$, at 4 °C was monitored over time by SLS. (b–d) DLS measurement of dominant particle sizes in the mixtures (defined as the size of a particle with the volume percentage >85%).

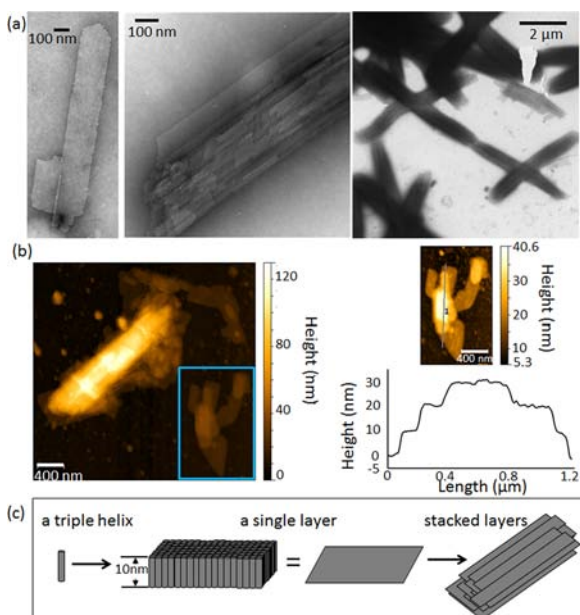


Figure 5. Sheet morphology. (a) TEM and (b) AFM of a 1:1 L to D mixture. Contour heights varied by integer multiples of 10 nm. (c) A proposed model of assembly where triple helices align into a 10 nm thick layer, which further stack. Samples were incubated at 4 °C for ~4 weeks prior to imaging.

opposite-handed threads.⁵ Several sheets were observed to stack in multilayered structures. Small ~100 nm particles were found in mixtures where the D-proline enantiomer was depleted (Figure S4).

Requirement of triple helices. The melting temperatures of $(L)P(L)PG)_{10}$ and $(D)P(D)PG)_{10}$ are ~25 °C (Figure S2). Assembly at temperatures below, at, and above the melting temperature was characterized to test the contribution of triple-helix unfolding. Turbidity was observed after incubation at 4, 25, and 40 °C for 3 days (Figures 6, 7a). At this time point, the 25 °C structures were micrometer-sized sheets. Assembly of 4 °C structures was slower, with uniform ~100 nm particles observed after 3 days. It took over a month for micrometer-scale sheets to form at 4 °C (Figure 5). Aggregation was also observed at high temperature (40 °C). However, the assembly at 40 °C showed different features such as

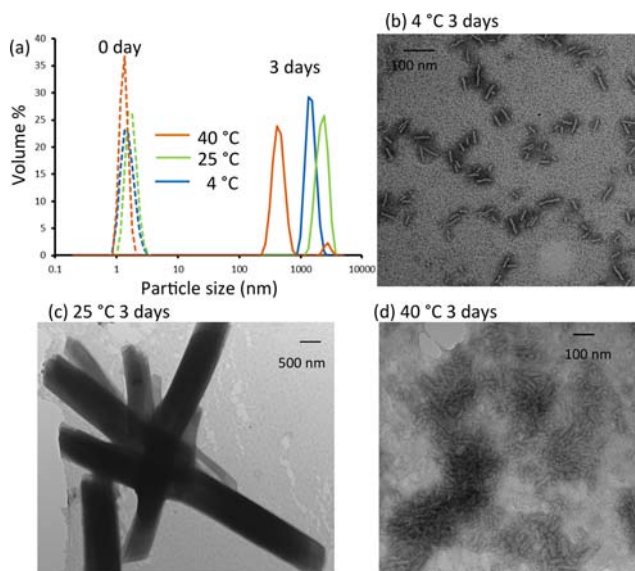


Figure 6. Influence of temperature on sheet morphology. (a) Particle size distribution in 1:1 mM of $(L)P(L)PG)_{10}$ and $(D)P(D)PG)_{10}$ mixture detected with DLS at 0 and 3 days incubation at 4, 25, and 40 °C, respectively. (b–d) TEM samples prepared under the same condition as in DLS.

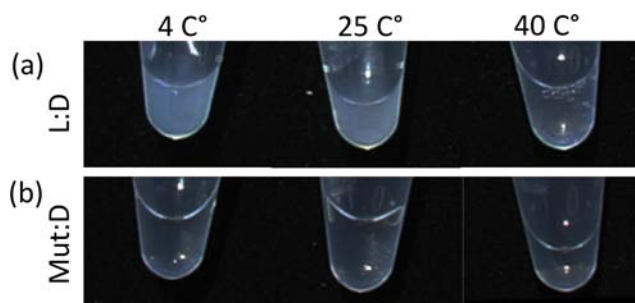


Figure 7. Folding of the triple-helix required for assembly. Photographs of (a) L:D = 1 mM $(L)P(L)PG)_{10}$: 1 mM $(D)P(D)PG)_{10}$. (b) D:Mut = 1 mM $(D)P(D)PG)_{10}$: 1 mM mutant-L. The samples were incubated at 4, 25, and 40 °C, respectively, for 3 days.

less turbidity, more irregular morphology, and much smaller sizes in a majority of the particles detected with DLS (Figures 6, 7a). This assembly may be caused by nonspecific interactions in the unfolded state although it is interesting to note that similar aggregates were not observed for L or D peptides alone.

To further clarify the importance of a folded triple-helix in driving supramolecular assembly, we designed a mutant L-peptide, $(L)P(L)PG)_{4L}P(L)P(L)P(L)PG)_{5}$, by removing a conserved glycine in the fifth triplet. This type of mutation has been shown to prevent triple helical formation.²² No triple helix was observed in the mutant peptide as evidenced by a lack of positive ellipticity at 225 nm in the circular dichroism spectrum (Figure S5). Mixtures of the mutant L-peptide and $(D)P(D)PG)_{10}$ remained transparent and soluble regardless of the incubation temperature (Figure 7b). Disrupting triple-helix folding of one of the components was sufficient to prevent sheet formation.

Interhelical distances. Computational simulations predict close packing of left-/right-handed triple-helix pairs. The crystalline sheets formed during self-assembly suggest a uniform supramolecular structure. Wide-angle X-ray scattering (WAXS) was used to characterize peptide organization.^{15,23,24} WAXS profiles confirmed the existence of triple helices and allowed us

to compare interhelical distances between homo- and heterochiral associations.

The diffraction patterns of the heterochiral sample showed three peaks: two overlapping peaks at ~ 13 Å and a third peak at ~ 11 Å. Such peak locations are typical of triple-helix equatorial peaks (13.7, 13.3, and 12.6 Å) found in natural collagen²⁵ (also see Table S2 and references therein). The absence of the 2.86 Å meridional reflection,²³ which is a strong indication for a triple helix, is due to the anisotropic nature of the sample.

Clear differences in interhelical distances of (PPG)₁₀ were observed between homochiral vs heterochiral assemblies. Since we were unable to induce the homochiral association under the same concentration as the heterochiral mixture (2 mM), an oversaturated (L₁PG)₁₀ suspension (~ 80 mM) was prepared to promote homochiral packing. The water content of the homochiral suspension was lower or similar to the heterochiral mixture. Even though drying of the samples may decrease their interhelical distances (Table S2 and references therein), the heterochiral mixture with higher water content still showed tighter packing than the homochiral one. The two interhelical distances of (L₁PG)₁₀ were both slightly larger than those of the (L₁PG)₁₀:(D₁PG)₁₀ mixture. These experimental differences in the interhelical distances were consistent with the computationally predicted ones (Table S1).

The mutant L-peptide showed a diffraction pattern lacking any peak characteristic of triple-helix formation within the 10–13 Å region (Figure 8), consistent with circular dichroism (Figure S5).

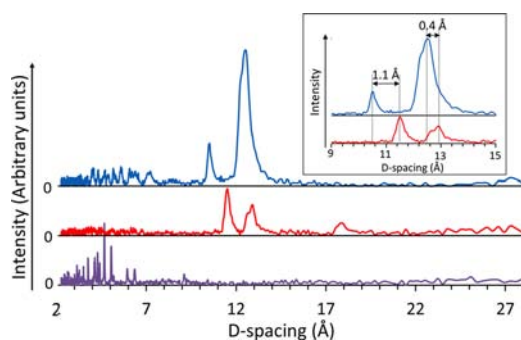


Figure 8. *D*-spacing measured with WAXS of mixture 1 mM (L₁PG)₁₀:1 mM (D₁PG)₁₀ (upper) compared to oversaturated (L₁PG)₁₀ suspension (middle) and oversaturated mutant L-peptide suspension (bottom). The *d*-spacing differences are shown in the inset.

The numerous sharp peaks between 2 and 7 Å in the mutant sample were observed instead of an intense broad peak at 4.5 Å that is typical of native collagen.²³ This suggests that the mutant L-peptide is highly crystalline but does not fold into triple helices.

In conclusion, using (PPG)₁₀ sequence enantiomers as minimal helical exemplars, the geometric prediction of preferred left-/right-handed helical pairings appears to hold true. However, even this system is complicated by chemical detail. In a series of experiments pairing (D₁PG)₁₀ with other right-handed triple-helical peptides such as (POG)₁₀, no interactions were observed. Hydroxylation of the proline side chain may sterically prevent close association of left- and right-handed species, increase the desolvation barrier required to allow tight ridges-in-grooves packing, or even modify the degree of supercoiling of the triple-helix such that different pitch of left- and right-handed species could preclude a coherent, columnar interaction. Ironically, this general rule of helix–helix association may best apply in special cases where complete mirror symmetry exists.

■ ASSOCIATED CONTENT

Supporting Information

Experimental methods and figures and tables. This material is available free of charge via the Internet at <http://pubs.acs.org>.

■ AUTHOR INFORMATION

Corresponding Author

nanda@cabm.rutgers.edu

Notes

The authors declare no competing financial interest.

■ ACKNOWLEDGMENTS

This work was supported by NIH DP2 OD-006478 and NIH R01 GM-089949. We thank Hiroshi Matsui for access to AFM.

■ REFERENCES

- (1) Woodhead-Galloway, J. *Acta Crystallogr., Sect. B* **1976**, *32*, 1880.
- (2) Straley, J. P. *Phys. Rev. A* **1976**, *14*, 1835.
- (3) Chothia, C.; Levitt, M.; Richardson, D. *J. Mol. Biol.* **1981**, *145*, 215.
- (4) Sia, S. K.; Kim, P. S. *Biochemistry* **2001**, *40*, 8981. Nanda, V.; DeGrado, W. F. *J. Am. Chem. Soc.* **2006**, *128*, 809.
- (5) Boncheva, M.; Bruzewicz, D. A.; Whitesides, G. M. *Langmuir* **2003**, *19*, 6066.
- (6) Fuhrhop, J.-H.; Krull, M.; Büldt, G. *Angew. Chem., Int. Ed. Engl.* **1987**, *26*, 699.
- (7) Saghatelian, A.; Yokobayashi, Y.; Soltani, K.; Ghadiri, M. R. *Nature* **2001**, *409*, 797.
- (8) Gerber, D.; Shai, Y. *J. Mol. Biol.* **2002**, *322*, 491.
- (9) Chung, D. M.; Nowick, J. S. *J. Am. Chem. Soc.* **2004**, *126*, 3062.
- (10) Ramagopal, U. A.; Ramakumar, S.; Mathur, P.; Joshi, R.; Chauhan, V. S. *Protein Eng.* **2002**, *15*, 331.
- (11) Milton, R. C.; Milton, S. C.; Kent, S. B. *Science* **1992**, *256*, 1445.
- (12) Pentelute, B. L.; Gates, Z. P.; Tereshko, V.; Dashnau, J. L.; Vanderkooi, J. M.; Kossiakoff, A. A.; Kent, S. B. *J. Am. Chem. Soc.* **2008**, *130*, 9695. Patterson, W. R.; Anderson, D. H.; DeGrado, W. F.; Cascio, D.; Eisenberg, D. *Protein Sci.* **1999**, *8*, 1410. Zawadzke, L. E.; Berg, J. M. *Proteins* **1993**, *16*, 301.
- (13) Lee, C. H.; Singla, A.; Lee, Y. *Int. J. Pharm.* **2001**, *221*, 1. O'Grady, J. E.; Bordon, D. M. *Adv. Drug Delivery Rev.* **2003**, *55*, 1699.
- (14) Rele, S.; Song, Y.; Apkarian, R. P.; Qu, Z.; Conticello, V. P.; Chaikof, E. L. *J. Am. Chem. Soc.* **2007**, *129*, 14780.
- (15) O'Leary, L. E. R.; Fallas, J. A.; Bakota, E. L.; Kang, M. K.; Hartgerink, J. D. *Nat. Chem.* **2011**, *3*, 821.
- (16) Kar, K.; Amin, P.; Bryan, M. A.; Persikov, A. V.; Mohs, A.; Wang, Y.-H.; Brodsky, B. *J. Biol. Chem.* **2006**, *281*, 33283.
- (17) Cejas, M. A.; Kinney, W. A.; Chen, C.; Vinter, J. G.; Almond, H. R., Jr.; Bals, K. M.; Maryanoff, C. A.; Schmidt, U.; Breslav, M.; Mahan, A.; Lacy, E.; Maryanoff, B. E. *Proc. Natl. Acad. Sci. U.S.A.* **2008**, *105*, 8513. Kar, K.; Ibrar, S.; Nanda, V.; Getz, T. M.; Kunapuli, S. P.; Brodsky, B. *Biochemistry* **2009**, *48*, 7959.
- (18) Przybyla, D. E.; Chmielewski, J. J. *Am. Chem. Soc.* **2008**, *130*, 12610.
- (19) Berisio, R.; Vitagliano, L.; Mazzarella, L.; Zagari, A. *Protein Sci.* **2002**, *11*, 262.
- (20) Nanda, V.; DeGrado, W. F. *J. Am. Chem. Soc.* **2005**, *128*, 809.
- (21) Okuyama, K.; Morimoto, T.; Narita, H.; Kawaguchi, T.; Mizuno, K.; Bachinger, H. P.; Wu, G.; Noguchi, K. *Acta Crystallogr., Sect. D* **2010**, *66*, 88.
- (22) Long, C. G.; Braswell, E.; Zhu, D.; Apigo, J.; Baum, J.; Brodsky, B. *Biochemistry* **1993**, *32*, 11688.
- (23) Rich, A.; Crick, F. H. C. *J. Mol. Biol.* **1961**, *3*, 483.
- (24) Okuyama, K.; Xu, X.; Iguchi, M.; Noguchi, K. *Peptide Sci.* **2006**, *84*, 181. Przybyla, D. E.; Rubert Pérez, C. M.; Gleaton, J.; Nandwana, V.; Chmielewski, J. J. *Am. Chem. Soc.* **2013**, *135*, 3418.
- (25) Brodsky, B.; Eikenberry, E. F. In *Methods Enzymol.*; Leon, W. Cunningham, D. W. F., Eds.; Academic Press: Waltham, MA, 1982; Vol. 82, p 127.